

# Deformation of liquid-filled calcium alginate capsules in a spinning drop apparatus

Sabine Leick,<sup>\*a</sup> Stefan Henning,<sup>b</sup> Patrick Degen,<sup>a</sup> Dieter Suter<sup>b</sup> and Heinz Rehage<sup>a</sup>

Received 8th October 2009, Accepted 7th January 2010

First published as an Advance Article on the web 3rd February 2010

DOI: 10.1039/b921116k

This paper describes the mechanical properties of thin-walled, liquid-filled calcium alginate capsules by measuring the deformation of these particles in a spinning drop apparatus. By variation of the guluronic acid content of the alginate, the polymerization time and the calcium and alginate concentration we systematically studied the elastic properties of these capsules. In a series of experiments we observed for the first time new types of irreversibly deformed capsules, which can be described by plastic deformation. For comparison purposes, we also investigated liquid-filled calcium alginate particles in squeezing capsule experiments. The qualitative and quantitative results of both experiments in terms of the deformation properties and the surface Young moduli were in good agreement. Furthermore we also investigated liquid-filled calcium alginate particles by NMR microscopy to characterize the capsules in view of their membrane thickness. These results, in combination with the spinning capsule experiments allowed us to measure the kinetics of surface gelation and the mechanism of membrane growing.

## 1. Introduction

Microcapsules are commonly used in pharmaceutical or medical processes for transporting drugs or encapsulation of organic cells.<sup>1–3</sup> Liquid-filled microcapsules consist of a liquid core surrounded by a thin, semi-permeable membrane.<sup>1,3</sup> The main functions of these membranes are the successful encapsulation, transportation and controlled release of the capsule content into the external environment. These properties depend crucially on the nature of the membrane structure.<sup>4</sup> Thereby, it is important that the thin-walled and fragile capsules do not break up when it is not supposed to. On the grounds of their limited stability, it is very interesting to study and characterize the deformation of capsules under the onset of mechanical forces. Compared with calcium alginate beads, investigations of liquid-filled calcium alginate capsules are very limited up to now.

In recent years different techniques have been proposed to measure capsule deformability. There is one, which consists of squeezing the capsules between two parallel plates under a given squeezing force.<sup>5</sup> In biochemistry the micropipette-technique is often used.<sup>6</sup> Here, the cell membrane is partial aspirated into a micropipette under a given pressure. Other methods are based on capsule deformations which are induced by viscous forces exerted by a flowing fluid.<sup>5,7</sup> Large capsules, as in this case, can be investigated in a spinning-drop apparatus.<sup>8,9</sup> As presented in this work, we study the deformation and elastic properties of single liquid-filled calcium alginate capsules under the action of centrifugal forces. For comparison

purposes, we also investigated these liquid-filled calcium alginate particles in squeezing capsule experiments.<sup>10,11</sup>

The size of the capsules and the thickness of the capsule walls are measured by NMR microscopy (microimaging). Compared to earlier techniques,<sup>12</sup> which consisted of cutting the capsules into halves and examining the membranes with a microscope, NMR microscopy is a more reliable and non-invasive method. Performing these measurements as a function of the polymerization time and the calcium as well as the alginate concentration provides information on the polymerization process. In recent years, this method was already used for studying the gelation process and structure of alginate beads and microcapsules<sup>13–15</sup> and it was also successfully applied in order to determine the thickness of poly-L-lysine layers on microcapsules.<sup>16</sup>

Of all different natural polymers that can be applied for the formation of semipermeable membranes, alginate is one of the most frequently used owing to the fact that its gelation is carried out under very mild conditions. Alginate shows a high biocompatibility and a total lack of toxicity.<sup>17,18</sup> On grounds of these outstanding properties alginates have been widely used in the food industry as thickening, stabilizing, gelling and film forming agents.<sup>19,20</sup>

The capsule membrane consists of alginate, a natural linear polysaccharide, extracted from marine brown algae. This macromolecule contains subunits of  $\beta$ -D-mannuronic and  $\alpha$ -L-guluronic acid. These monomers are arranged in a pattern of blocks along the chain with homo-polymeric regimes (termed M and G blocks).<sup>18,21,22</sup>

By cross-linking alginate chains with bivalent cations (Fig. 1), in this case calcium ions, three-dimensional isotropic gels are formed. The cross-linking process occurs by incorporation of  $\text{Ca}^{2+}$ -ions into the zigzag structure of the G-blocks (egg-box model).<sup>19,23,24</sup> The length of the G blocks is the main structural feature contributing to gel formation and gel strength.<sup>18</sup>

<sup>a</sup> Department of Physical Chemistry II, Technische Universität Dortmund, 44227 Dortmund, Otto-Hahn-Straße 6, Germany. E-mail: sabine.leick@tu-dortmund.de; Fax: 0049-(0)231-7555367; Tel: 0049-(0)231-7555030

<sup>b</sup> Department of Experimental Physics III, Technische Universität Dortmund, 44227 Dortmund, Otto-Hahn-Straße 4, Germany

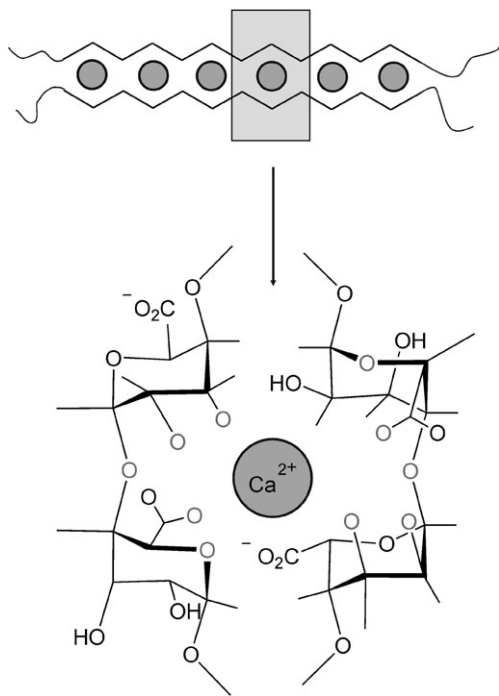


**Fig. 1** Schematic drawing of the egg-box model for alginate gel formation.<sup>18</sup>

## 2. Experimental

### 2.1 Capsule preparation

Liquid-filled calcium alginate capsules were prepared by extrusion, using a simple one-step process.<sup>25,26</sup> Sodium alginates MANUCOL DM and MANUGEL DMB (G39 and G63) were purchased from ISP, Germany. Sodium alginate solutions of different concentrations were used for the preparation of the capsules.

For preparing the cross-linking aqueous  $\text{Ca}^{2+}$ -solutions,  $\text{CaCl}_2 \cdot 2\text{H}_2\text{O}$  salt was first dissolved in double distilled water. Droplets of this  $\text{CaCl}_2$  solution were then added drop-wise through a syringe into a cylindrical glass filled with 25 ml of sodium alginate solution. A capsule membrane was formed instantly around each droplet as the two liquids came into contact. Because the calcium cation has a smaller size than the large polymer molecules it can diffuse into the alginate solution, and according to the egg-box model this leads to cross-linking processes. Induced by these diffusion processes the gel membrane grows along the flux direction of the calcium ions.<sup>12</sup>

In order to avoid the aggregation of the prepared capsules, the sodium alginate solution was constantly agitated using a magnetic stirrer placed at the bottom of the reaction vessel. A dropping height of 5 cm was used to ensure that spherical capsules were formed. After a certain gelation time the capsules were separated, filtered and washed with double distilled water. This process removes the alginate solution outside the formed capsules and reduces the possibility of capsules sticking together when they are in close contact. After isolating the capsules they were immediately transferred into a 1.5% wt  $\text{CaCl}_2 \cdot 2\text{H}_2\text{O}$  solution with the aim of stabilizing the calcium alginate membranes and completing the polymerization process.<sup>27</sup>

The produced and characterized liquid-filled alginate capsules exhibit diameters of round about 2.3 mm and membrane thicknesses in the range of 80  $\mu\text{m}$  up to 210  $\mu\text{m}$  depending on the polymerization time.

### 2.2 Three dimensional gel layer preparation

Three dimensional alginate gels were prepared in order to investigate the existence of irreversible plastic deformation processes of the capsule membranes. For establishing comparability between the capsule membranes and the three-dimensional alginate gel layers, the concentrations were adjusted to obtain the same gel composition. The three-dimensional gel layers were formed by mixing 50 ml of a 1% wt alginate solution with 50 ml of a 0.78% wt  $\text{CaCO}_3$  (MERCK, Germany) suspension under stirring. Then 1.211 g glucono delta-lactone (GDL), a naturally-occurring food additive, dissolved in 5 ml of water and purchased from MERCK, Germany as well, was added. The gelation was initiated by the release of calcium ions caused by slow reactions of the  $\text{CaCO}_3$  crystals with the weak acid GDL.<sup>28</sup> After stirring the mixture for some minutes the obtained solutions were filled in small and flat plastic vessels.

After one hour the gels were characterized by rheological measurements using stress ramp tests. For these experiments we used an advanced rheometric expansion system (ARES) from TA Instruments with plate/plate geometry. The upper titanium-plate had a diameter of 25 mm.

### 2.3 Spinning capsule experiments

A commercial spinning drop video tensiometer SVT 20 from Dataphysics was used to study the deformation properties of alginate capsules. A schematic drawing of such an apparatus is shown in Fig. 2. For these kind of measurements the capsule is assumed to be a sphere in its quiescent state. It is filled with an incompressible liquid with density  $\rho_i$  (aqueous  $\text{CaCl}_2$  solution) and is enclosed by an infinitely thin-walled elastic membrane. The capsule was placed inside the cylindrical rotating tube, which was filled with the outer phase, another incompressible liquid, with density  $\rho_e$  (FC 70: perfluorotripropylamine and isomers), whereas  $\rho_e > \rho_i$ .

By closing the tube, special caution was necessary to avoid air bubbles and dust particles. After insertion of the tube in the measuring cell, the deformation experiments were started by rotating the cylindrical tube around the direct axis with steady angular velocity  $\omega$ . Because of the high centrifugal forces, the capsule was centered on the tube axis. At experimental conditions an initially spherical alginate capsule could be deformed by increasing the rotation speed of the glass tube, as shown in Fig. 3. The maximum operating speed of the glass capillary was limited to 10 000 rpm. Above this value, vibrations became important, and leaking occurred from sealing. Each time before starting a new experiment, the rotating tube was cleaned with acetone for several times.

The shape and size of the capsules was recorded by means of a CCD-camera and the deformation was calculated by a special program automatically. The optical distortions due to the lens effects of the glass tube and to the refractive indices of the solvents were compensated by the computer program as

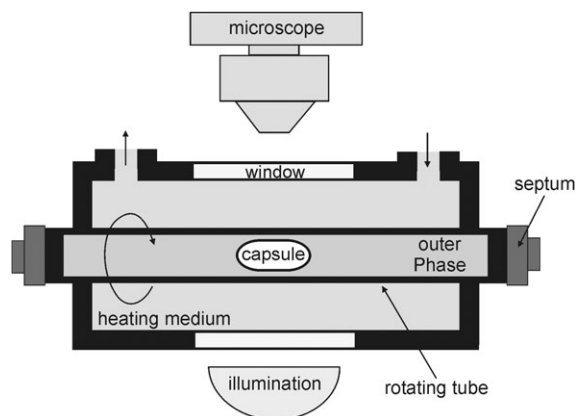


Fig. 2 Schematic drawing of a spinning-drop tensiometer.<sup>9</sup>

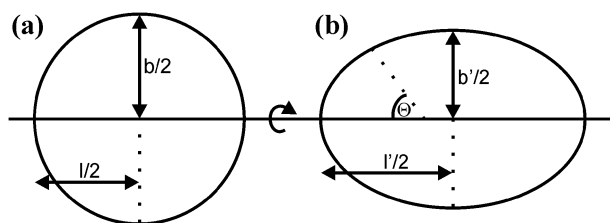


Fig. 3 Schematic drawing of capsule deformation: (a) undeformed spherical initial state; (b) deformed elliptical final state of the capsule.

well. The overall deformation  $D$  of the capsules calculated by the results of the contour analysis is defined as:<sup>8,9</sup>

$$D = \frac{(l - b)}{(l + b)} \quad (1)$$

where  $l$  and  $b$  denotes the length and width of the capsule profile. A convenient way to express the result is to compute the difference between the final ( $D$ ) and initial ( $D_0$ ) deformation of the capsules:

$$\Delta D = D - D_0 \quad (2)$$

A detailed description of the theory of spinning capsule experiments is represented in ref. 8 and 9. In the linear viscoelastic regime, the capsule deformation can be described by:

$$D = -\Delta\rho\omega^2a^3 \frac{(5 + \nu_s)}{16E_s} \quad (3)$$

In this equation,  $\Delta\rho$  denotes the density difference between the internal and external liquid,  $a$  is the radius of the capsules in the quiescent state,  $\omega$  describes the angular velocity of tube rotation,  $E_s$  is the surface Young modulus and  $\nu_s$  the surface Poisson ratio. Eqn (3) predicts that the capsule deformation depends on the ratio  $(5 + \nu_s)/16E_s$ , and that it is not possible to obtain separately the values of the surface Young modulus and the surface Poisson ratio from the spinning capsule experiments. However,  $D$  is not very sensitive to the exact value of the surface Poisson ratio when the latter varies between  $-1$  and  $1$ . On this grounds, eqn (3) can approximately be used to calculate membrane elastic properties from spinning capsule experiments.

## 2.4 NMR microscopy measurements

The membrane thicknesses of differently prepared liquid-filled calcium alginate capsules were determined by NMR microimaging measurements. The capsules were placed into a 5 mm NMR tube which contained a two-phase liquid system. The lower phase in the tube consisted of tetrachloroethylene and filled the lowest 2 cm of the tube. This solution was covered with a 2 cm layer double distilled water including 0.5% wt  $\text{CaCl}_2$  and a small amount of  $\text{CuSO}_4$ . The paramagnetic  $\text{Cu}^{2+}$  shortens the  $T_1$ -relaxation of the surrounding water and helps to reduce the time needed for the microimaging experiments by allowing short repetition times. A two-phase system was chosen to allow positioning of the capsules at the phase border. Since the highest point of the interface between the two liquids was at the center of the tube, the capsules were pushed to a stable position at the edge of the tube. At the bottom of the glass, in a system without tetrachloroethylene, the discontinuity of susceptibility at the interfaces of air, glass and water distorts the local homogeneity of the magnetic field.

To determine the thickness of the capsule membranes, a spin-echo imaging sequence (also known as spin-warp<sup>29</sup>) was used. The measurements were done on a Chemagnetics Infinity Plus 600 spectrometer, equipped with a microimaging accessory, consisting of a Bruker Microimaging Probehead inserted in a Resonance Research BFG-73/45-100 MK 2 gradient unit. The images were obtained with a field of view (FOV) of  $6 \times 6 \text{ mm}^2$  and a slice thickness of  $100 \mu\text{m}$ . 256 phase-encoding steps were performed, each with an acquisition length of 256 points, which leads to a resolution of  $23 \mu\text{m}$ . 8 scans were accumulated for each phase-step to improve the signal-to-noise ratio. The echo-time was 14 ms, the repetition time was 1 s and the total duration of the experiment was about 35 min.

After the acquisition of the NMR image, the thickness of the capsule was determined by measuring the distance of two contour levels at 50% of the signal maximum. This measurement was repeated at several positions and of 5 capsules for each polymerization time and concentration and the results were averaged.

## 2.5 Squeezing capsule experiments

To investigate the mechanical stability of liquid-filled calcium alginate capsules with different guluronic acid concentrations, we squeezed single capsules between two parallel plates (Fig. 4).<sup>10,11</sup> For these experiments we used an ARES from TA Instruments with plate/plate geometry. The upper titanium-plate had a diameter of 25 mm. The resulting normal force was measured by a force rebalance transducer with normal force (FRTN 1) with a measuring range between 2 gmF and 2000 gmF ( $1.96 \times 10^{-2} \text{ N}$  to 19.6 N).

We used a force gap test to compress the capsules from 1 mm to 0.01 mm during 360 s with a logarithmical decreasing compression rate. During the compression experiments we measured the gap and the normal force at the upper plate simultaneously. Each measurement was repeated three times. We present the mean values with the standard deviation, respectively. The normal force (in mN) versus the gap distance (in mm) results in typical compression curves.<sup>30,31</sup> From these curves we obtained first of all qualitative differences in the

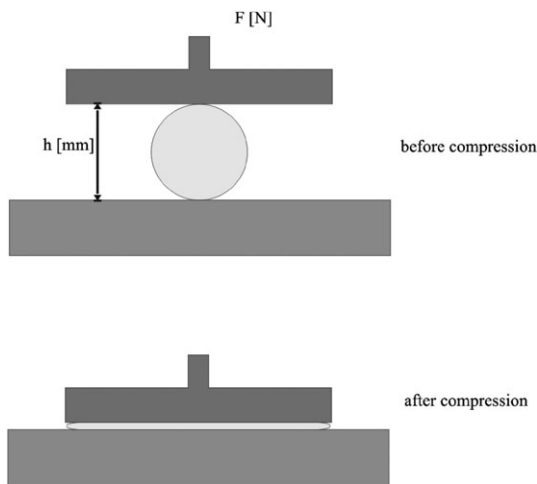


Fig. 4 Schematic drawing of the capsule compression.

mechanical stability between the synthesized capsules. Furthermore the surface Young modulus can be calculated by a quantitative analysis of the obtained force-displacement curves by different methods of resolution.<sup>11,32,33</sup>

In earlier studies we used this technique to investigate the mechanical stability of ionotropic alginate beads.<sup>34</sup>

### 3. Results and discussions

#### 3.1 Alginate capsules with different guluronic acid concentrations

The composition and block structure of alginate molecules depend on the algae source and tissue. These parameters are important for the gel formation of the alginates.<sup>35</sup> As the junction zones are only formed in blocks of guluronic acid (egg-box-model), it is interesting to analyze the influence of the chemical composition on the capsule stability. In a series of experiments we observed that a larger  $\alpha$ -L-guluronic acid content (G63) leads to a lower capsule deformability (Fig. 5).

This is due to the fact that more junction zones are available in the G63 alginate, so that a mechanically stronger gel is formed. For low centrifugal forces we did not detect significant changes of deformation, whereas at higher angular velocities the  $\Delta D$  (the difference between the final ( $D$ ) and initial ( $D_0$ ))

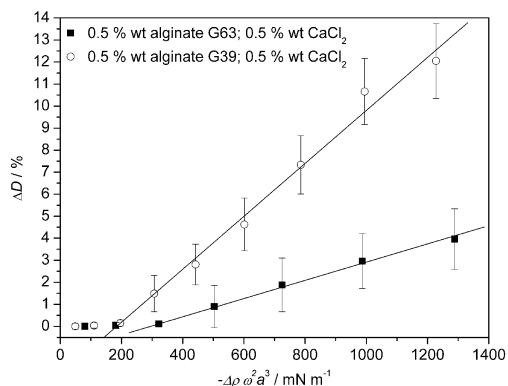


Fig. 5 Deformability of liquid-filled calcium alginate capsules with different guluronic acid contents as a function of  $-\Delta\rho\omega^2a^3$ .

deformation of the capsules) increased. At  $1200 \text{ mN m}^{-1}$  we obtained typical deformations of about 12% for capsules made of G39 alginate. In comparison, alginate G63 capsules only showed deformations of about 6%. These capsule membranes seemed to be much stronger and stiffer than those formed by the alginate G39.

It is interesting to note that a certain force has to act on the capsules before the deformation starts to increase at all. For the capsules made of alginate G39 this needed force effect, as shown in Fig. 5, is significantly lower than for the capsules made of alginate G63. If the membrane is purely elastic, the deformation should linearly increase with the strength of the centrifugal field. In former investigations, we measured this typical behavior for aminomethacrylate and organosiloxane microcapsules.<sup>8,9</sup> The data obtained for alginate membranes are completely different. It is evident, that a threshold value of the centrifugal force is needed to induce capsule deformations. After exceeding this limiting force, the particle deformation increases approximately linearly as a function of the centrifugal force.

Based on these results, eqn (3) can be modified to obtain deformation results of different alginate capsules. Due to the fact that the linear increase with the strength of the centrifugal field starts after achieving the threshold value, it is necessary to add a constant term for the negative axis intercept:

$$D = \Delta\rho\omega^2a^3 \frac{(5 + \nu_s)}{16E_s} - Y_V \quad (4)$$

where  $Y_V$  describes the yield value in percent. Eqn (4) makes it possible to calculate the surface Young modulus of the two different capsule types shown in Fig. 5. Assuming a value for the Poisson ratio of  $\frac{1}{3}$ , we obtain for the capsules formed by alginate G39 a value of  $2.8 \text{ N m}^{-1}$  and for the capsules formed by alginate G63 a value of  $11.3 \text{ N m}^{-1}$ .

To illustrate the significant differences in the deformability of alginate capsules we present some pictures taken by the camera of the spinning-drop apparatus for different angular velocities (Fig. 6). The horizontal line represents the axis of symmetry of the tube. As already mentioned, a higher  $\alpha$ -L-guluronic acid content (G63) affects a significant lower capsule deformability.

The deformations of liquid-filled calcium alginate capsules seem to be irregular and unusual, if we compare the distorted capsule profiles with shapes of other common particles like acrylate or polysiloxane capsules.<sup>8,9</sup> For alginate capsules we did not obtain an ellipsoidal deformation structure by increasing the tube rotation. We observed, instead, an abnormal deformed structure which was stretched to both sides. The center of the capsules, however, remained approximately ellipsoidal. This observation points to the presence of plastic membrane deformations, which occur after exceeding the threshold or yield value. This is consistent with the observation, that the capsule deformations were not completely reversible. Fig. 7 shows that the capsules remain permanently deformed after increasing and reducing the rotational speed.

From theoretical arguments, the membrane stresses attain greatest values at the end caps, and bursting processes always take place in these regions.<sup>8,9</sup> We can, hence, expect that irreversible plastic deformation processes mainly occur at

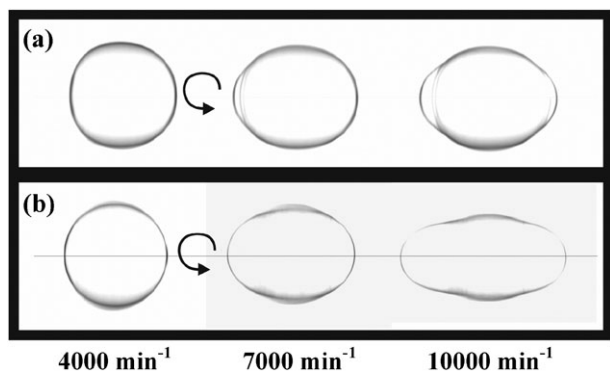


**Fig. 6** Unusual alginate capsule shapes for different guluronic acid concentrations at various rotational speeds (a) alginate G63 (b) alginate G39.

these parts of the capsules. This is consistent with the experimental observations.

In order to explore that plastic membrane deformations are responsible for the threshold value of the centrifugal force we performed rheological tests on three-dimensional gel layers. In a series of experiments we measured the steady-state values of the deformation  $\gamma$  of three dimensional, thin alginate gel layers (in the region of 3 mm) as a function of the applied shear stress  $\sigma$ .

These experiments can be compared with the capsule membranes because the compositions of the alginate gels were identical. As shown in Fig. 8, the stress ramp test approves the existence of a yield stress for the measured alginate gel layer. For the G63 alginate gel, the shear stress which is needed to initiate the plastic gel deformation is much higher than for G39 alginate gel. This is consistent to the results measured by the spinning drop apparatus (Fig. 5). We can explain these results by assuming a higher cross-linking density of the gel containing more guluronic acid groups.

In addition, we noticed that the deformation of the calcium alginate capsules was not always symmetrically performed at both sides of the capsules. This can be explained by the presence of small membrane defects, which evidently lead to preferred deformation processes. Summarizing all performed

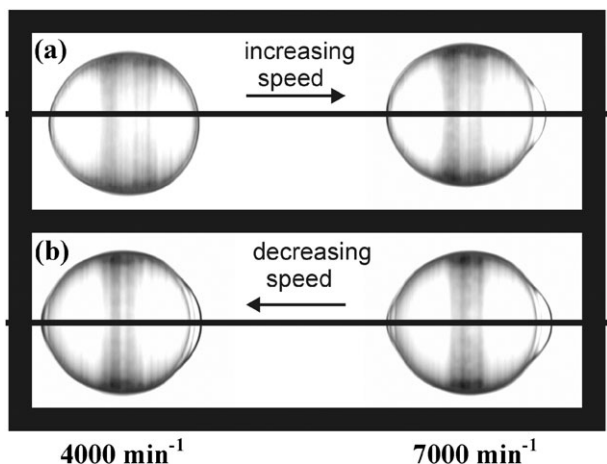


**Fig. 7** Irreversibility of capsule deformation (a) by increasing and (b) decreasing the rotating speed.

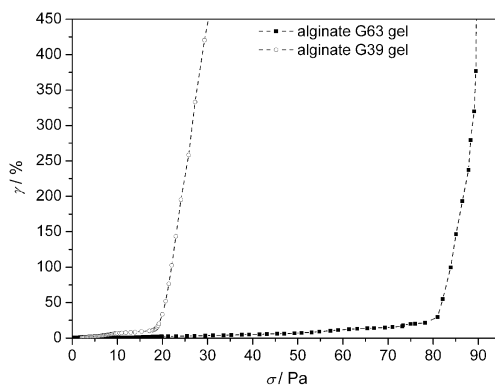


**Fig. 8** Stress ramp test of two different alginate gels with the same composition as the comparable calcium alginate capsule membranes.

measurements we may state that the liquid-filled alginate capsules show new types of complicated shape transitions. These phenomena can be traced back to plastic deformations and non-linear constitutive laws of the enclosing membranes.

A series of different capsules was also investigated in squeezing capsule experiments. This method is particularly useful to explore qualitative differences in the mechanical stability of the alginate membranes. Typical results of such measurements are summarized in Fig. 9a. It is evident that alginate G63 capsules are more stable than alginate G39 particles. These results are consistent with the data obtained in the spinning capsule measurements.

For obtaining quantitative results, an analysis of the compression curves in Fig. 9b by eqn (5) provides the two-dimensional Young modulus  $E_s$  in the range of small deformations under point loading close to the pole by a simple linear fit:<sup>32</sup>

$$F = \frac{4E_s d}{a\sqrt{3(1-\nu^2)}} d_D \quad (5)$$

In this equation,  $d$  denotes the membrane thickness,  $a$  is the radius of the capsule,  $d_D$  is the displacement of the capsule pole,  $F$  is the measured force,  $E_s$  is the surface Young modulus and  $\nu_s$  the surface Poisson ratio for which a value of  $\frac{1}{3}$  was assumed. As mentioned before, other more complicated methods of resolution by dissolving numeric calculations are presented in further citations.<sup>11,33</sup> Eqn (5) only holds in the regime of very small deformations of the spherical capsules.

For the capsule squeezing experiments we obtained a surface Young modulus of  $6.5 \text{ N m}^{-1}$  for the alginate G39 capsules, and we measured  $32.9 \text{ N m}^{-1}$  for the alginate G63 capsules. It is evident, that the results of spinning capsule and compression experiments are in general agreement. Both experiments are sensitive enough to characterize the mechanical behavior of the liquid-filled alginate capsules. It was explicitly shown that the guluronic acid content of the alginate had a significant influence on the deformability and mechanical strength of the capsule walls.

In further experiments we performed rheological frequency sweep tests on three-dimensional gel layers. Relevant results are summarized in Fig. 10. It is easy to see that the storage modulus is much larger than the loss modulus. The gel layers are mainly characterized by elastic properties. The slow

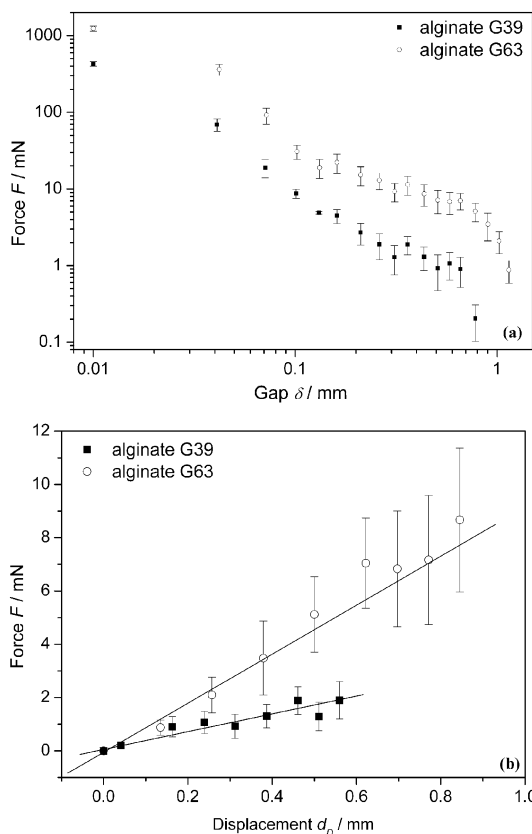


**Fig. 9** Force-gap curves (a) and force-displacement curves (b) of two different types of liquid-filled calcium alginate capsules. Influence of the guluronic acid concentration on the capsule stability (G39 compared with G63 capsules of equal size and shape).

decrease of the moduli as a function of the angular frequency point to the existence of relaxation processes, which can be induced by the release of entrapped entanglements or the opening of ionic junction points. These phenomena are not very pronounced, and the gels mainly exhibit rubber-elastic properties. If the measured three-dimensional moduli are multiplied with the thickness of the gel layers, we obtain the two-dimensional properties of these viscoelastic gels. For the alginate gel G63 we obtained a Young modulus of  $35.2 \text{ N m}^{-1}$  and for the alginate gel G39 we calculated  $7.5 \text{ N m}^{-1}$ . These data, which are summarized in Table 1, are in good agreement with the results of the capsule squeezing experiments.

The results of the spinning capsule experiments, are generally a factor of two or three lower. This could be explained by the fact that the centrifugal force may have an influence on the cross-linking process of the alginate membranes.

### 3.2 Capsule deformability as a function of the calcium and alginate concentration

In a series of experiments we also varied the calcium and alginate concentrations. Typical results of these measurements are represented in Fig. 11. It is shown in Fig. 11a and b that the deformation increases with growing angular velocity for all capsules. An increase of the calcium counter-ion concentration leads to the formation of stiffer and stronger membranes; that means the cross-linking density increases. Enhanced stability

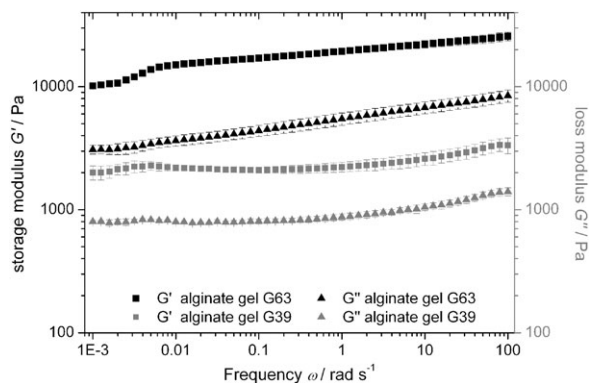


**Fig. 10** Frequency sweep tests of two different alginate gels (bulk phase) with the same composition as the comparable calcium alginate capsule membranes ( $\text{gap}_{\text{G39}} = 2.5 \text{ mm}$ ;  $\text{gap}_{\text{G63}} = 3.2 \text{ mm}$ ).

**Table 1** The surface Young moduli for the two gels measured with different experimental techniques, assuming a poisson ratio of  $\frac{1}{3}$

Gel	G39	G63
Spinning capsule experiment	$2.8 \text{ N m}^{-1}$	$11.3 \text{ N m}^{-1}$
Capsule squeezing experiment	$6.5 \text{ N m}^{-1}$	$32.9 \text{ N m}^{-1}$
Rheology	$7.5 \text{ N m}^{-1}$	$35.2 \text{ N m}^{-1}$

can also be induced by using elevated alginate concentrations (Fig. 11b). The spinning capsules experiments are suitable for measuring the deformation of liquid-filled calcium alginate capsules under variation of the concentrations. For production processes, these parameters must be optimized in order to synthesize tailor-made capsules of desired sizes and shapes. Especially the variation of the calcium concentration often implies problems. If the polymerization kinetics is too fast, one does not obtain spherical capsules. In opposition, the decrease of the calcium concentrations leads to the formation of thin-walled membranes. These particles are elongated and damaged by the stirring process.

### 3.3 Influence of the gelation time on the deformation behavior of alginate capsules

For capsules made of 0.5% wt alginate G63 and 0.5% wt  $\text{CaCl}_2$  we measured the capsule deformation as a function of the gelation time. As shown in Fig. 12, an increase of the polymerization time up to 180 s causes a significant decrease of the deformation. This phenomenon can be explained by the formation of an elevated number of junction points which lead to a higher gel strength. In the range between 180 s and 270 s we did not observe considerable changes, which lead to the assumption that after this time span all existing calcium ions are incorporated in the zigzag blocks of the alginate.

The kinetics of capsule gelation is also represented in Fig. 13. In this diagram we investigated the capsule deformation for different rotational speeds as a function of the gelation time. The data can roughly be described by curves of single exponential decay. This means, that the gelation process follows first order kinetics. This occurs because the initial

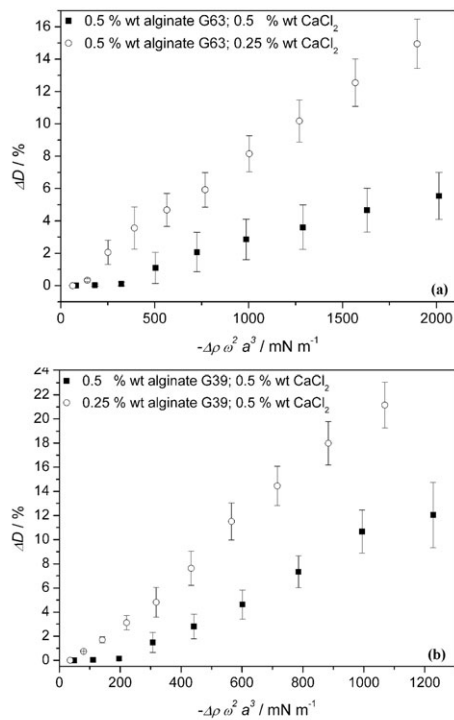


**Fig. 11** Spinning capsule experiments of liquid-filled calcium alginate capsules under variation of the (a) calcium and (b) alginate concentration.

molar concentration of the calcium ions is much larger than the concentration of alginate molecules (pseudo first order kinetics). At these conditions, the surface Young modulus  $E_s$  can be described by:

$$E_s(t) = E_s(\infty)(1 - \exp(-kt)) \quad (6)$$

In this equation,  $E_s(\infty)$  describes the elastic membrane properties after infinite gelation time (equilibrium modulus). The constant  $k$  denotes the rate constant of the surface polymerization. As the surface Young modulus is proportional to the density of junction points (theory of rubber-like elasticity), the curves of Fig. 13 describe the evolution of cross-linking points during the process of surface gelation.

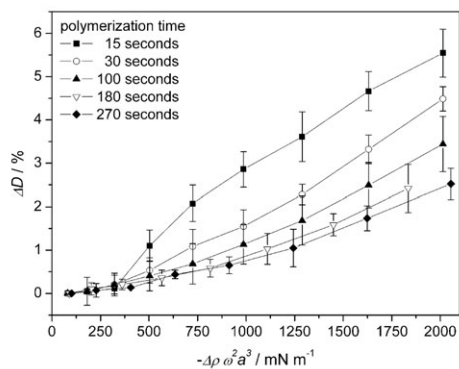


**Fig. 12** Capsule deformation as a function of  $-\Delta\rho\omega^2a^3$  for different gelation times.

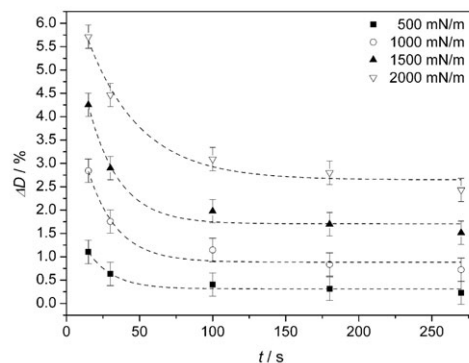


**Fig. 13** Capsule deformation as a function of the gelation time for different centrifugal forces.

Most probably, the rough approximation of the curve fitting adapted to the obtained measuring data points to a gelation kinetics which is not purely diffusion controlled. This notice leads to the assumption that there are other processes, such as reorientation of the alginate chains or ionic interactions caused by positive charge preponderance, which have an effect on calcium alginate gel formation.

### 3.4 Membrane thicknesses measured by NMR microscopy

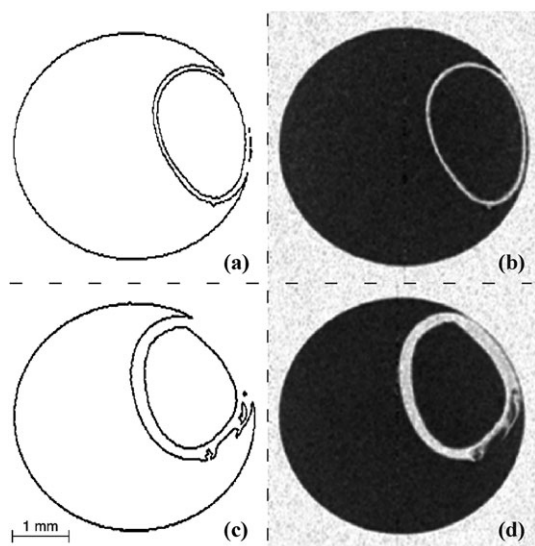
Fig. 14 shows two examples of NMR microscopy images, which were used to determine the membrane thickness of different liquid-filled calcium alginate capsules. The slices are 100  $\mu\text{m}$  thick, perpendicular to the NMR sample tube, whose inner diameter is 4.24 mm. The upper half of the figure shows a capsule prepared with a polymerization time of 15 s. Its membrane is  $78 \pm 7 \mu\text{m}$  thick. If the polymerization time is increased to 180 s (lower part), the thickness increases to  $202 \pm 13 \mu\text{m}$ .

Fig. 15 shows the dependence of the membrane thickness on the gelation time. For these measurements, the concentrations of the sodium alginate (G63) and calcium chloride solution were both 0.5% wt. The increase of the membrane thickness is significant at small gelation times and slower at longer gelation times. This is consistent to the increasing diffusion resistance and decreasing calcium chloride concentration.

Blandino *et al.*<sup>12</sup> obtained nearly the same curve progression for the thickness of gel layer capsules as a function of time for a different alginate capsule system, considerably higher concentrations and measured by cutting the capsules into halves and examining the membranes with a microscope. The curve in Fig. 15 was obtained by fitting the experimental data to the binomial diffusion equation:<sup>12,36</sup>

$$V = V_{\max}[1 - \exp(-kt)]^n \quad (7)$$

In this equation,  $k = 0.004 \text{ s}^{-1}$  and  $n = 0.3$  denote the gelation rate constant and the heterogeneous structural resistance constant, respectively. The heterogeneous structural resistance constant of 0.4 consolidates the assumption that further processes, in addition to the diffusion, have an effect on the calcium alginate gel formation and consequently on the gelation kinetics.



**Fig. 14** NMR Images of two capsules: (a) contour plot of a capsule with a polymerization time of 15 s and (c) 180 s; (b) and (d) grayscale plots of the same capsules.

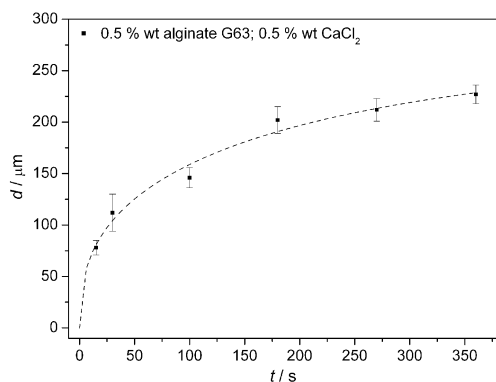


**Fig. 15** Membrane thickness as a function of polymerization time.

Fig. 16a depicts the influence of the calcium as well as the alginate concentration (Fig. 16b) on the membrane thickness. Fig. 16a illustrates that the thickness of the alginate gel membranes increases with the calcium concentration, whereas the alginate concentration does not show an effect on the thickness.

Summing up, the NMR microscopy is well suited for measuring the membrane thickness of liquid-filled calcium alginate capsules. The dependence of the membrane thickness on the polymerization time is consistent with the time dependence of the deformational properties. In both cases, it is demonstrated explicitly that the diffusion of the calcium ions into the environmental alginate solution controls the representative deformational and mechanical properties. At a high calcium concentration gradient, and therefore at the beginning of the polymerization and for small polymerization times, the changes in the membrane thickness, as well as in the deformation are high. For long polymerization times, the gradient becomes smaller and thus the changes decrease up to a plateau value. At this point, we assume that all available calcium ions are linked into the emerging gel network.

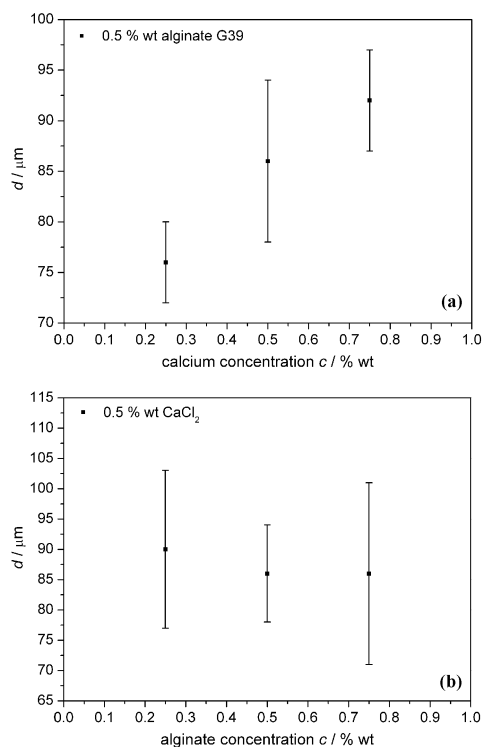


**Fig. 16** Membrane thickness as a function of the (a) calcium chloride and (b) sodium alginate G39 concentration at a polymerization time of 15 s.

## 4. Conclusion

In this paper we studied the mechanical properties of thin-walled, liquid-filled calcium alginate capsules. We measured the deformation of these particles in a commercial spinning drop video tensiometer. In a series of measurements we analyzed the elastic properties of these capsules by varying the guluronic acid content of the alginate, the gelation time and the calcium as well as the alginate concentration. The experiments showed that an increasing amount of  $\alpha$ -L-guluronic acid leads to higher cross-linked samples. This can be explained by the fact that more junction zones were produced leading to mechanically stronger gel shells. We approved this observation by additional squeezing capsule experiments, which showed the same results.

In addition, we detected new and unusual capsule shapes, which were formed by plastic membrane deformations. The application of external forces leads to breaking processes of junction points, which are responsible for the existence of a threshold value. Furthermore, stress ramp tests of different alginates showed that for a stronger cross-linked gel network, caused by elevated guluronic acid concentration, a higher force is needed to transform the gel into a fluid state.

In further experiments we investigated the influence of the calcium and alginate concentration on the capsule deformability. An increase of the polysaccharide or counter-ion concentration results in the formation of more elastic capsule shells. By variation of the concentrations it is, however, more complicated to form spherical particles. It is interesting, to note, that the variation of the alginate concentration did

not show an effect on the membrane thickness, and the deformational properties were not influenced directly by the membrane thickness.

The kinetics of the surface gelation was first investigated by spinning capsule experiments. Up to a certain reaction time there is a decrease of the deformability, which is consistent with the formation of a higher density of cross-linking points and therefore higher gel strength. The cross-linking process of the alginate shells can approximately be described by first order kinetics. The plateau value describes the equilibrium structure where the number of junction points remains stable. The rough description of time dependent experiments leads to the assumption that the gelation kinetics is not purely diffusion controlled. There may be other processes, such as reorientation of the alginate chains, ionic interactions or cooperative processes of the extended ionic junction zones which have an effect on the calcium alginate gel formation. In combination with the squeezing capsule test, the spinning capsule experiments allowed us to characterize the mechanical properties of thin-walled calcium alginate capsules. Similar investigations can also be used to characterize liquid-filled pectin capsules. Such experiments are currently performed in our institute.

By comparing the kinetics of surface gelation with the evolution of the membrane thickness, we obtained similar results. In both cases, it was demonstrated that the diffusion of the calcium ions mainly controls the mechanical properties and the membrane thickness of the capsules. Besides these phenomena also more complicated cross-linking processes were presented.

The surface Young moduli, which were measured by three different methods, are at least of the same order of magnitude. We can use these experimental methods of rheology, spinning and squeezing capsule experiments in order to achieve comparable information on the elastic properties of cross-linked gel membranes.

## Acknowledgements

We acknowledge financial support by the German Research Foundation (DFG-Project Re 681/19-1). Furthermore we thank Mr. Wojciech Koziel for measuring the deformability of alginate capsules with different G-share with spinning-drop apparatus.

## References

- 1 J. M. Guisan, *Methods Biotechnol.*, 2006, **22**, 345–355.
- 2 S. H. Hu, C. H. Tsai, C. F. Liao, D. M. Liu and S. Y. Chen, *Langmuir*, 2008, **24**, 11811–11818.
- 3 L. Y. Chu, S. H. Park, T. Yamaguchi and S. Nakao, *Langmuir*, 2002, **18**, 1856–1864.
- 4 T. M. S. Chang, *Artificial Cells*, Thomas, Springfield, III, 1972.
- 5 K. S. Chang and W. L. Olbricht, *J. Fluid Mech.*, 1993, **250**, 587.
- 6 R. M. Hochmuth and R. E. Waugh, *Annu. Rev. Physiol.*, 1987, **49**, 209.
- 7 A. Walter, H. Rehage and H. Leonhard, *Colloid Polym. Sci.*, 2000, **278**, 167.
- 8 G. Pieper, H. Rehage and D. Barthès-Biesel, *J. Colloid Interface Sci.*, 1998, **202**, 293–300.
- 9 M. Husmann, H. Rehage, E. Dhenin and D. Barthès-Biesel, *J. Colloid Interface Sci.*, 2005, **282**, 109.
- 10 G. Sun and Z. Zhang, *Int. J. Pharm.*, 2002, **242**, 307–311.
- 11 M. Carin, D. Barthès-Biesel, C. Postel, F. Edwards-Lévy and D. C. Andrei, *Biotechnol. Bioeng.*, 2003, **82**, 207–212.
- 12 A. Blandino, M. Macias and D. Cantero, *J. Biosci. Bioeng.*, 1999, **88**, 686–689.
- 13 J. M. Duez, M. Mestdagh, R. Demeure, J. F. Goudemant, B. P. Hills and J. Godward, *Magn. Reson. Chem.*, 2000, **38**, 324–330.
- 14 B. P. Hills, J. Godward, M. Debatty, L. Barras, C. P. Saturio and C. Ouwerx, *Magn. Reson. Chem.*, 2000, **38**, 719–728.
- 15 B. Manz, M. Hillgärtner, H. Zimmermann, D. Zimmermann, F. Volke and U. Zimmermann, *Eur. Biophys. J.*, 2004, **33**, 50–58.
- 16 I. Constantinidis, S. C. Grant, S. Celper and I. Gauffin-Holberg, *Biomaterials*, 2007, **28**, 2438–2445.
- 17 A. C. Jen, M. C. Wake and A. G. Mikos, *Biotechnol. Bioeng.*, 1996, **50**, 357–364.
- 18 O. Smidsrød and G. Skjåk-Bræk, *Trends Biotechnol.*, 1990, **8**, 71–78.
- 19 A. Martinsen, I. Storror and G. Skjåk-Bræk, *Biotechnol. Bioeng.*, 1992, **39**, 186–194.
- 20 M. Indergaard and K. Østergaard, Polysaccharides for food and pharmaceutical uses, in *Seaweed Resources in Europe: Use and Potential*, ed. M. D. Gury and G. Blunden, John Wiley & Sons Ltd, Chichester, England, 1991, pp. 169–184.
- 21 Y. A. Mørch, I. Donati, B. L. Strand and G. Skjåk-Bræk, *Biomacromolecules*, 2006, **7**, 1471–1480.
- 22 R. M. Hassan, M. T. Makhlof and S. A. El-Shatoury, *Colloid Polym. Sci.*, 1992, **270**, 1237–1242.
- 23 A. Banerjee, D. Nayak and S. Lahiri, *Biochem. Eng. J.*, 2007, **33**, 260–262.
- 24 T. Chandy, D. L. Mooradian and G. H. R. Rao, *Artif. Organs*, 1999, **23**, 894.
- 25 S. C. Nigam, I. F. Tsoa, A. Sakoda and H. Y. Wang, *Biotechnol. Tech.*, 1988, **2**, 271–276.
- 26 Y. Chai, L. H. Mei, G. L. Wu, D. Q. Lin and S. J. Yao, *Biotechnol. Bioeng.*, 2004, **87**, 228–233.
- 27 Y. Chai, L. H. Mei, D. Q. Lin and S. J. Yao, *J. Chem. Eng. Data*, 2004, **49**, 475–478.
- 28 M. Wloka, *PhD dissertation*, University of Dortmund, Germany, 2006.
- 29 P. Callaghan, *Principles of Nuclear Magnetic Resonance Microscopy*, Oxford, 1991.
- 30 M. Rachik, D. Barthès-Biesel, M. Carin and F. Edwards-Lévy, *J. Colloid Interface Sci.*, 2006, **301**, 217–226.
- 31 F. Risso and M. Carin, *Phys. Rev. E: Stat., Nonlinear, Soft Matter Phys.*, 2004, **69**, 061601.
- 32 A. Fery and R. Weinkammer, *Polymer*, 2007, **48**, 7221–7235.
- 33 M. W. Keller and N. R. Sottos, *Exp. Mech.*, 2006, **46**, 725–733.
- 34 P. Degen, S. Leick and H. Rehage, *Z. Phys. Chem.*, 2009, **223**, 1079–1090.
- 35 E. Murano, *J. Appl. Ichthyol.*, 1998, **14**, 245–249.
- 36 K. Yamagiwa, Y. Shimizu, T. Kozawa, M. Onodera and A. Ohkawa, *J. Chem. Eng. Jpn.*, 1992, **25**, 723–728.